Supporting Information

Structural switching from paramagnetic to single-molecule magnet behaviour of $LnZn_2$ trinuclear complexes

Poh Ling Then,[a] Chika Takehara,[a] Yumiko Kataoka,[a] Motohiro Nakano,[b] Tomoo Yamamura,[c] and Takashi Kajiwara*[a]

a Faculty of Science, Nara Women's University, Nara, Nara 630-8506, Japan. Tel: +81-742-20-3402; E-mail: kajiwara@cc.nara-wu.ac.jp

b Graduate School of Science, Osaka University, Toyonaka, Osaka 560-0043, Japan.

c Institute for Materials Research, Tohoku University, Aoba-ku, Sendai, Miyagi 980-8577, Japan.

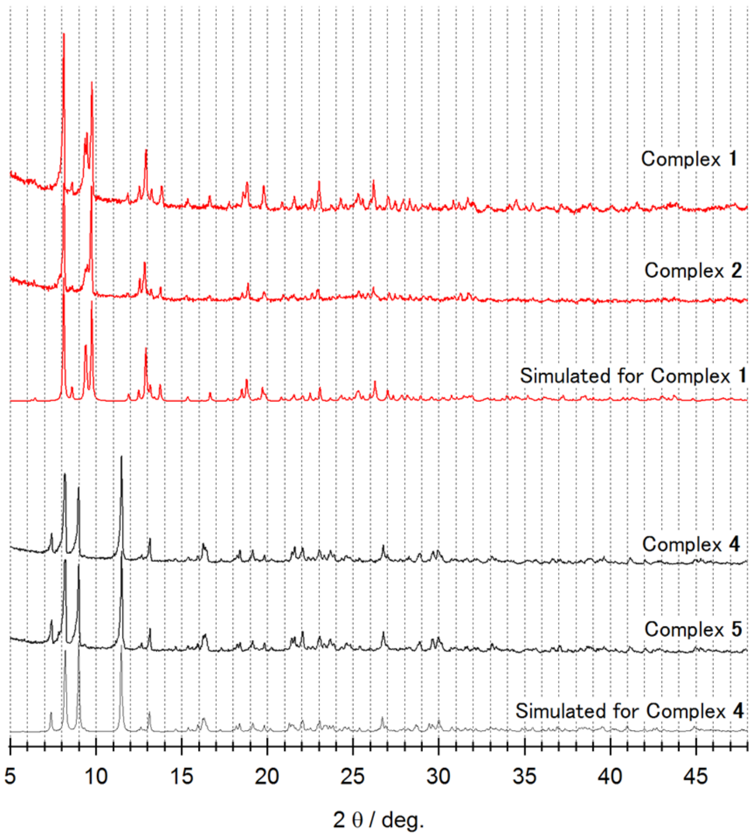

Figure S1 Powder X-ray diffraction data collected for Tb^{III} and Dy^{III} complexes **1**, **2**, **4**, and **5** at room temperature. Simulated patterns were calculated on the basis of the single-crystal X-ray crystallography results of complexes **1** in type-B structure and **4** in type-A structure, respectively.

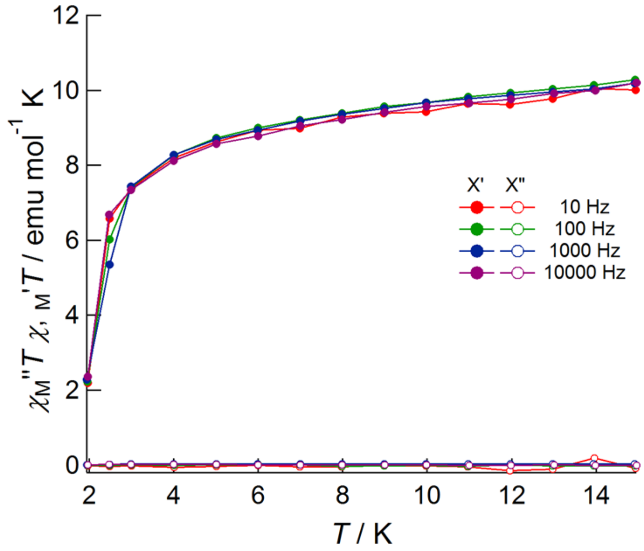

Figure S2 Temperature dependence of the products of in-phase and out-of-phase molar susceptibilities χ_M' and χ_M'' and temperature T of **1** measured under an oscillating field of 3 Oe with frequencies of 10, 100, 1000, and 10000 Hz under zero dc field.

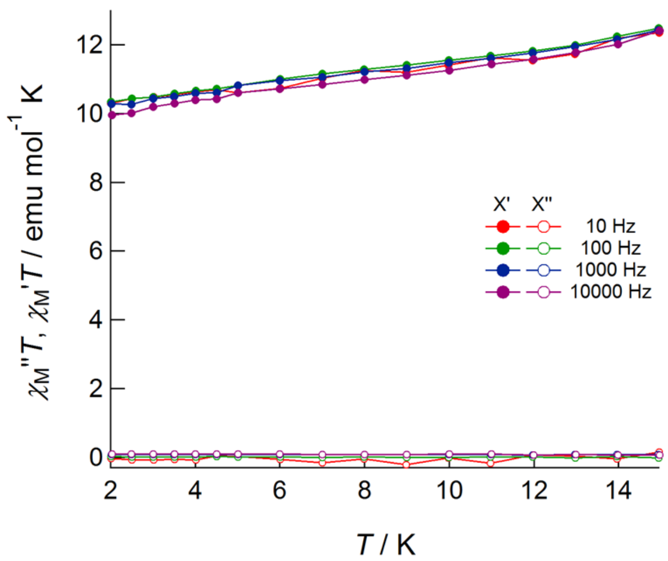

Figure S3 Temperature dependence of the products of in-phase and out-of-phase molar susceptibilities χ_M' and χ_M'' and temperature T of **2** measured under an oscillating field of 3 Oe with frequencies of 10, 100, 1000, and 10000 Hz under zero dc field

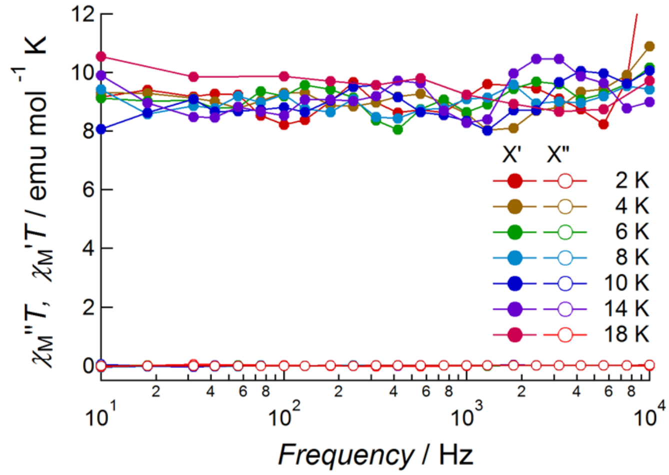

Figure S4 Frequency dependence of products $\chi_M'T$ (closed circle) and $\chi_M''T$ (open circle) of **4** measured at temperatures ranging from 2 to 18 K under an oscillating field of 3 Oe and an applied dc field of 0 Oe.

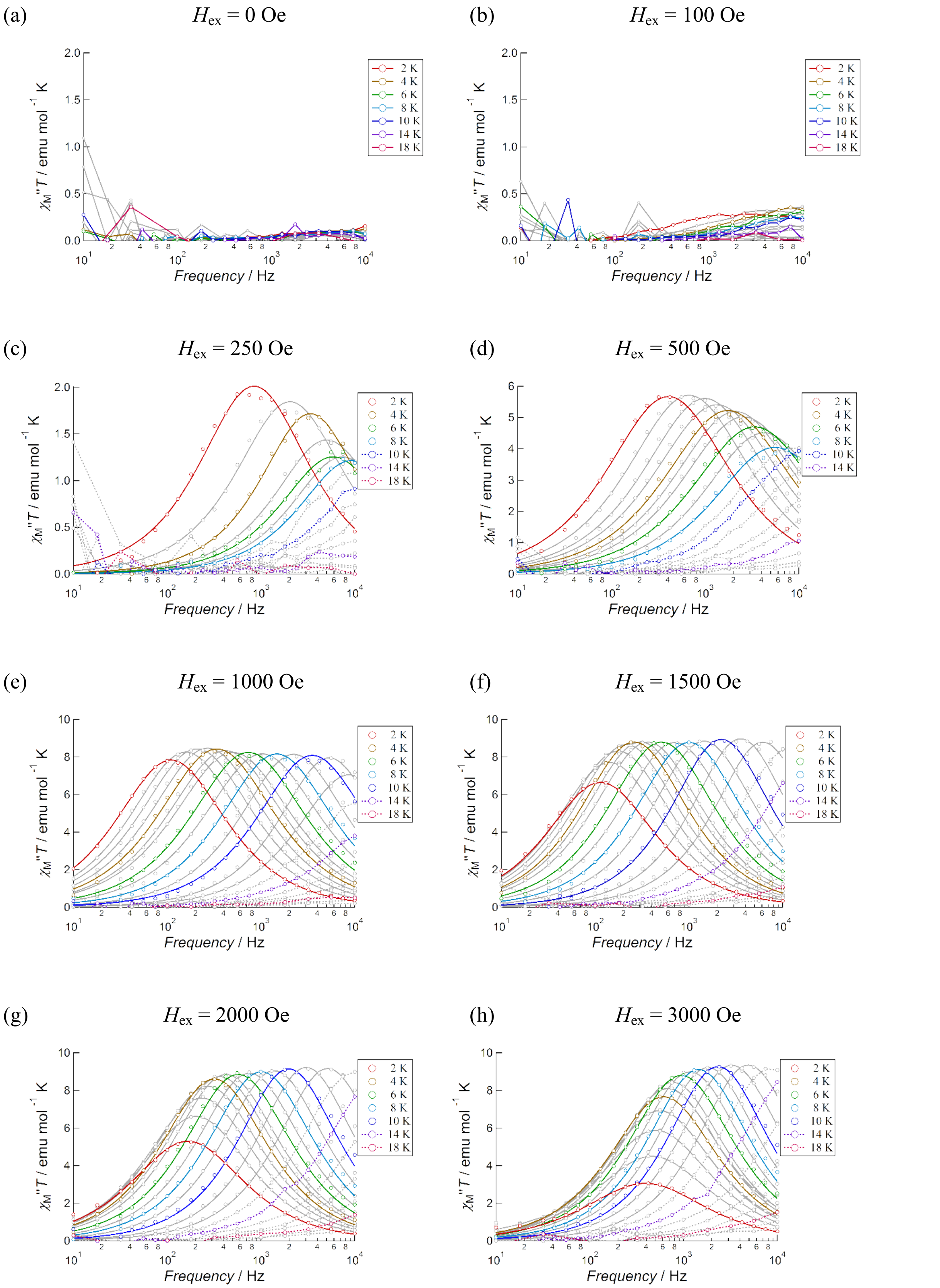

Figure S5 Frequency dependence of the product of χ_M'' and temperature of **4**, $\chi_M''T$, measured under 0-3000 Oe dc field. Solid curves for (a) and (b) are the guide for eyes. Solid curves for others represent the results of fits to a generalized Debye model, while the dotted curves are the guide for eyes.

(a) H_{ex} = 500 Oe

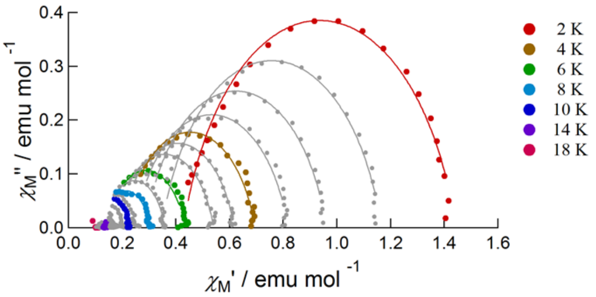

(b) H_{ex} = 1000 Oe

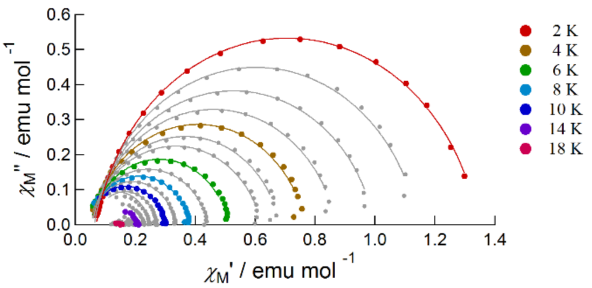

(c) H_{ex} = 1500 Oe

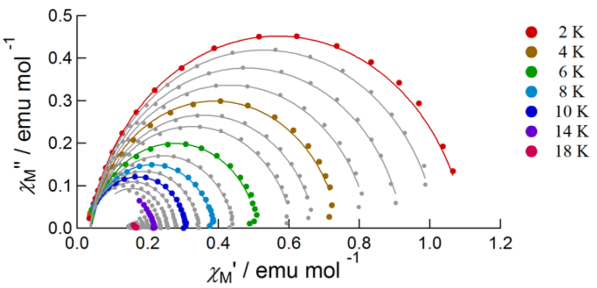

(d) H_{ex} = 2000 Oe

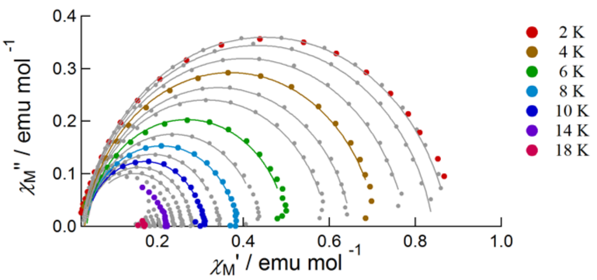

(e) H_{ex} = 3000 Oe

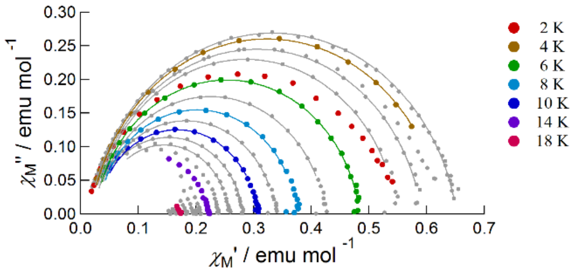

Figure S6 Cole-Cole plots of **4** measured under the application of external 500-3000 Oe dc field. Solid curves represent theoretical calculations on the basis of the generalized Debye model.

Table S1 Best fitted parameters of the extended Debye model for **4** under 1000 Oe dc field.

T/K	χ_T / emu mol^{-1}	χ_S / emu mol^{-1}	τ / s	α
2.0	9.891(15)	0.259(7)	0.001447(6)	0.113(2)
2.5	8.41(4)	0.47(2)	0.001010(12)	0.116(7)
3.0	7.35(3)	0.42(2)	0.000767(8)	0.132(6)
3.5	6.40(4)	0.40(3)	0.0005907(10)	0.136(10)
4.0	5.65(4)	0.38(4)	0.000469(11)	0.141(13)
4.5	5.03(4)	0.38(4)	0.000378(9)	0.143(15)
5.0	4.58(3)	0.35(4)	0.000317(7)	0.156(12)
6.0	3.76(4)	0.37(5)	0.000216(8)	0.13(2)
7.0	3.26(3)	0.33(3)	0.000155(3)	0.145(11)
8.0	2.804(14)	0.34(4)	0.000108(3)	0.120(15)
9.0	2.456(13)	0.35(3)	0.0000710(19)	0.096(12)
10.0	2.214(8)	0.27(5)	0.000045(2)	0.115(16)
11.0	1.975(7)	0.40(2)	0.0000298(8)	0.054(8)
12.0	1.817(14)	0.472(13)	0.0000181(4)	0.086(5)

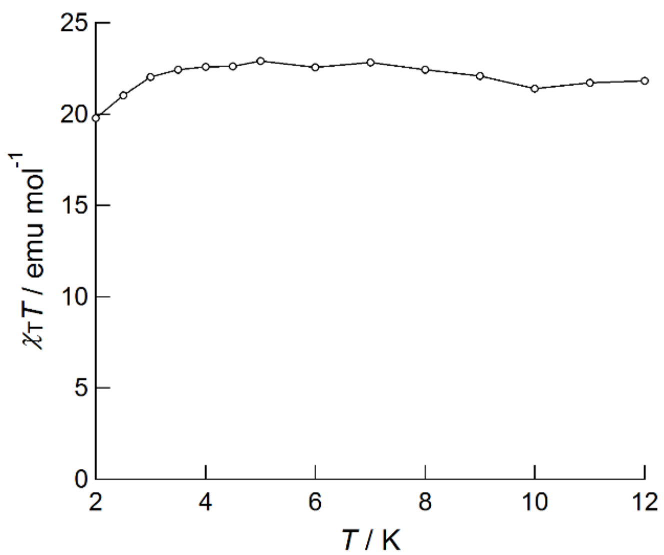

Figure S7 Temperature dependence of the product of the isothermal susceptibility χ_T and temperature T of **4** measured under 1000 dc field.

Detail of the Arrhenius analysis considering four relaxation processes

Both field and temperature dependence of τ^{-1} was analysed by equation 1.

$$1/\tau(H,T) = 1/\tau_{\text{Direct}}(H,T) + 1/\tau_{\text{Tunnel}}(H) + 1/\tau_{\text{Raman}}(T) + 1/\tau_{\text{TA-QTM}}(T)$$

$$= A_1 H^2 T + A_2 H^4 T + \frac{B_1}{1 + B_2 H^2} + CT^n + \tau_0^{-1} \exp(-\Delta E/k_B T) \quad (1)$$

In this equation, the first and second terms on the right side denote a direct process, the third term denotes the resonance tunnelling process, and the fourth and fifth terms represent the Raman and TA-QTM processes, respectively. To individually analyse the field and temperature dependence of τ^{-1}, T or H was fixed at the values of T_1 K or H_1 Oe to derive the following equations:

$$\tau(H,T_1)^{-1} = (A_1 H^2 + A_2 H^4)T_1 + \frac{B_1}{1 + B_2 H^2} + D_1 \quad \text{(S1)}$$

and

$$\tau(H_1,T)^{-1} = D_2 T + CT^n + \tau_0^{-1} \exp(-\Delta E/k_B T) + D_3 \quad \text{(S2)}$$

Here, constants D_1, D_2, and D_3 are expressed as

$$D_1 = CT_1^n + \tau_0^{-1} \exp(-\Delta E/k_B T_1) \quad \text{(S3)}$$

$$D_2 = A_1 H_1^2 + A_2 H_1^4 \quad \text{(S4)}$$

and

$$D_3 = \frac{B_1}{1 + B_2 H_1^2} \quad \text{(S5)}$$

The expected value of n is 7 for non-Kramers ions, 9 for Kramers ions, and 5 when two or more ground pairs of sub-levels are closely located or are degenerate.[16a] In this analysis, n was initially fixed at 7. Constant D_1 is independent of the field, while constants D_2 and D_3 are independent of temperature; however, they depend on each other in equation 1 and cannot be simultaneously estimated. Hence, a self-consistent analysis was employed to obtain the values of seven parameters of A_1, A_2, B_1, B_2, C, τ_0, and $\Delta E/k_B$. D_1 would be small at the lowest temperature (T_1 = 2.0 K); hence, we first assumed D_1 to be 0 for the analysis of the field dependence of τ^{-1} at 2.0 K to obtain the values of four parameters of A_1, A_2, B_1, and B_2 (Fig. 7 in main text). Using these values, constants D_2 and D_3 were calculated, and the temperature dependence of ln(τ/s) (Fig. 6 in main text, H_1 = 1000 Oe) was analyzed on the basis of equation S2, which gave values of three parameters of C, τ_0^{-1}, and $\Delta E/k_B$. Using the resultant values, D_1 was modified, and the field dependence of τ^{-1} was analyzed again to achieve better values for A_1, A_2, B_1, and B_2, and these cycles were repeated until all parameters became consistent.

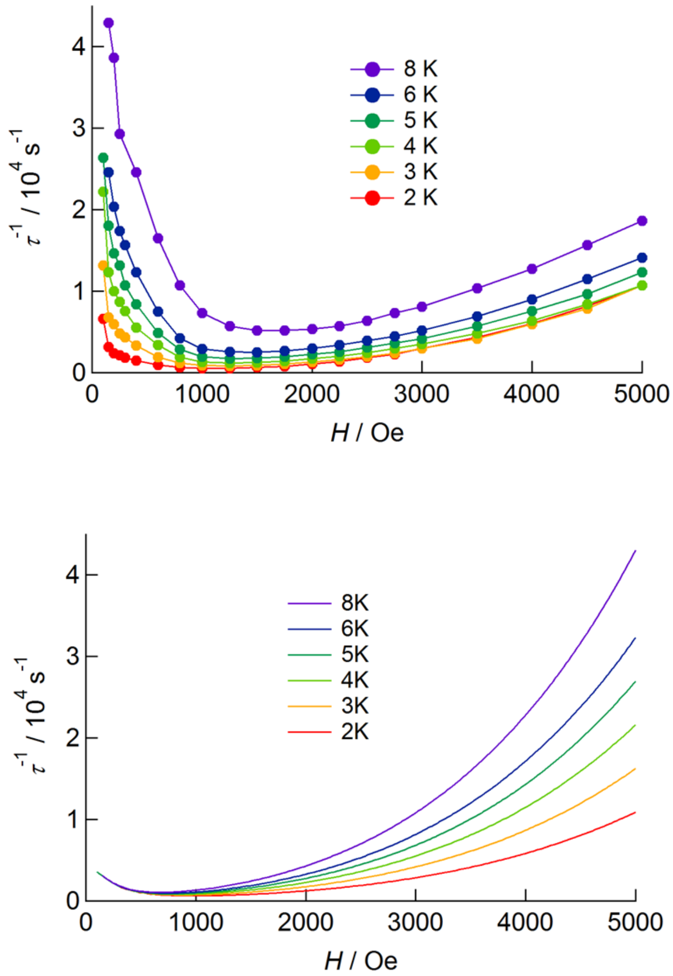

Figure S8 Dc field dependence of the relaxation rate τ^{-1} of **4** measured at several temperatures ranging from 2 K to 8 K. Top) observed data. Bottom) theoretical curves on the basis of the parameters of A_1 = 1.1(6) × 10^{-5} s^{-1} Oe^{-2} K^{-1}, A_2 = 4.2(3) × 10^{-12} s^{-1} Oe^{-4} K^{-1}, B_1 = 3.9(4) × 10^3 s^{-1}, B_2 = 1.5(3) × 10^{-5} Oe^{-2}, C = 14.3(8) × 10^{-4} K^{-7} s^{-1}, $\Delta E/k_B$ = 8.8 (4) K, τ_0 = 7.1(7) × 10^{-5} s, and n = 7.

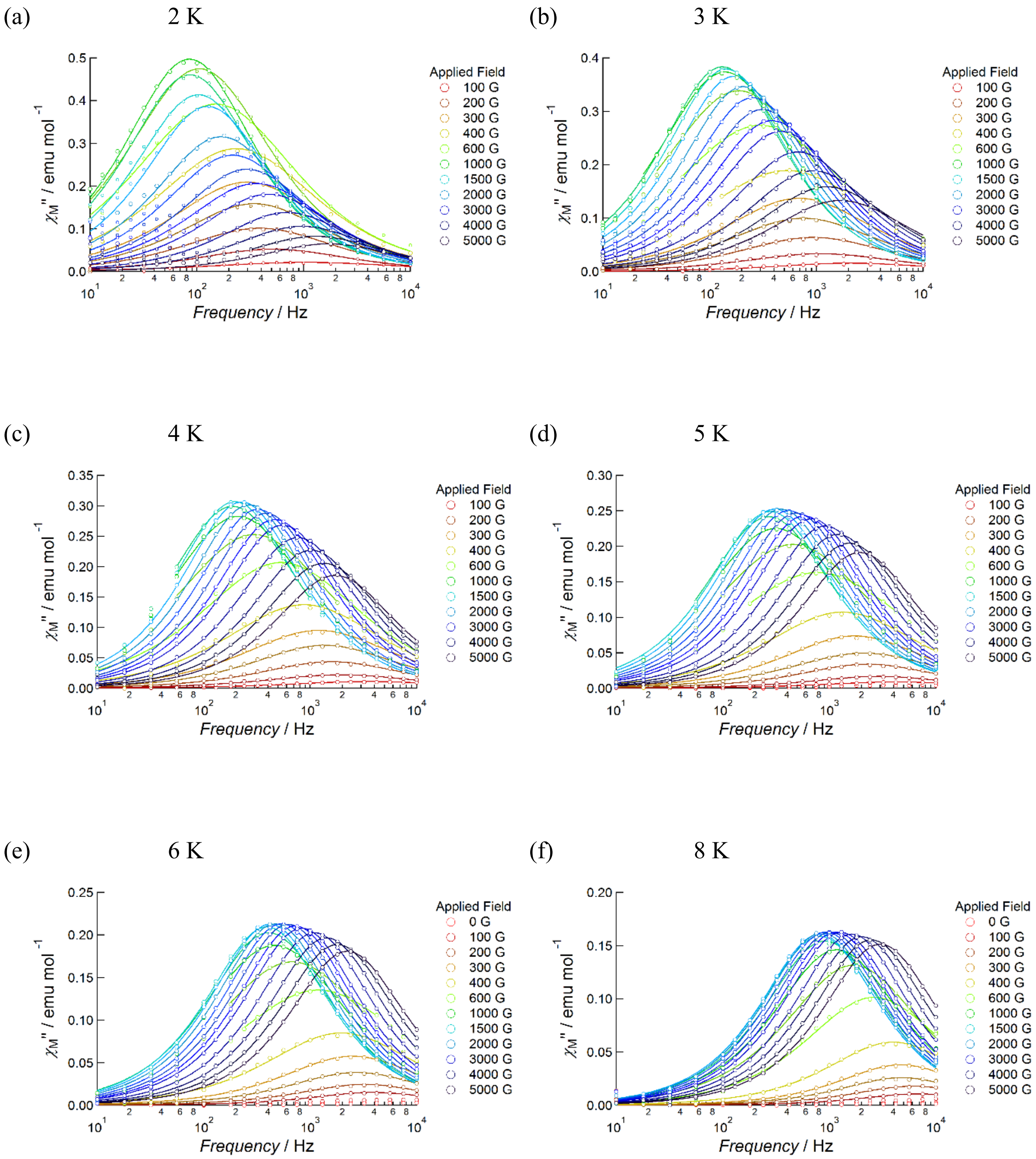

Figure S9 Dc field dependence of the χ_M'' of **4** measured at several temperatures ranging from 2 K to 8 K. Solid curves represent the results of fits to a generalized Debye model.

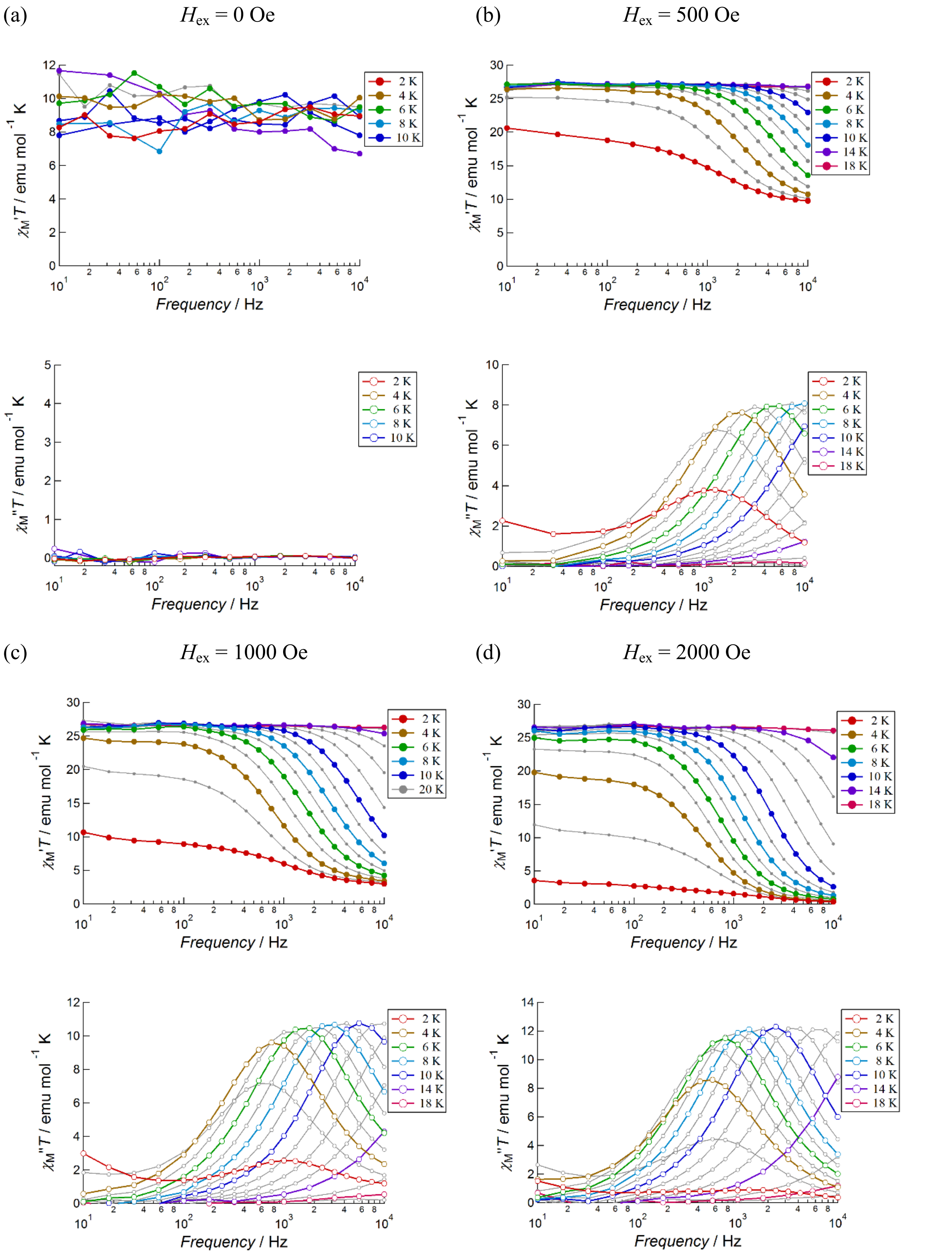

Figure S10 Frequency dependence of the products of $\chi_M'T$ (closed circles) and $\chi_M''T$ (open circles) of $[Tb(NO_3)\{Zn(L)(SCN)\}_2]$ (**4'**) in type-A structure, measured under 0-2000 Oe dc field. Solid curves are the guide for eyes.

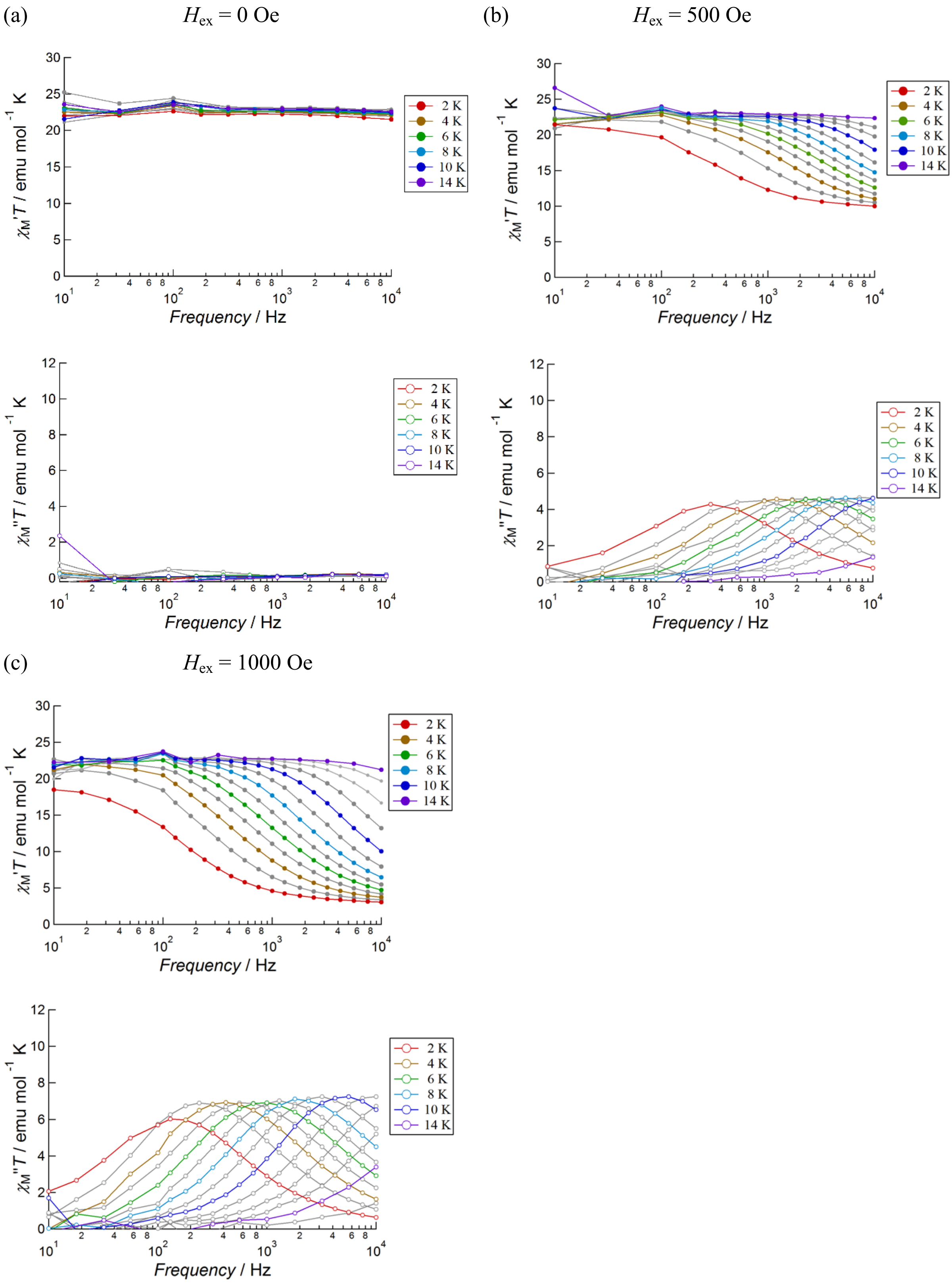

Figure S11 Frequency dependence of the products of $\chi_M'T$ (closed circles) and $\chi_M''T$ (open circles) of $[Tb_{0.07}La_{0.93}(NO_3)\{Zn(L)(SCN)\}_2]$ (**4''**) in type-A structure, measured under 0-1000 Oe dc field. Solid curves are the guide for eyes.

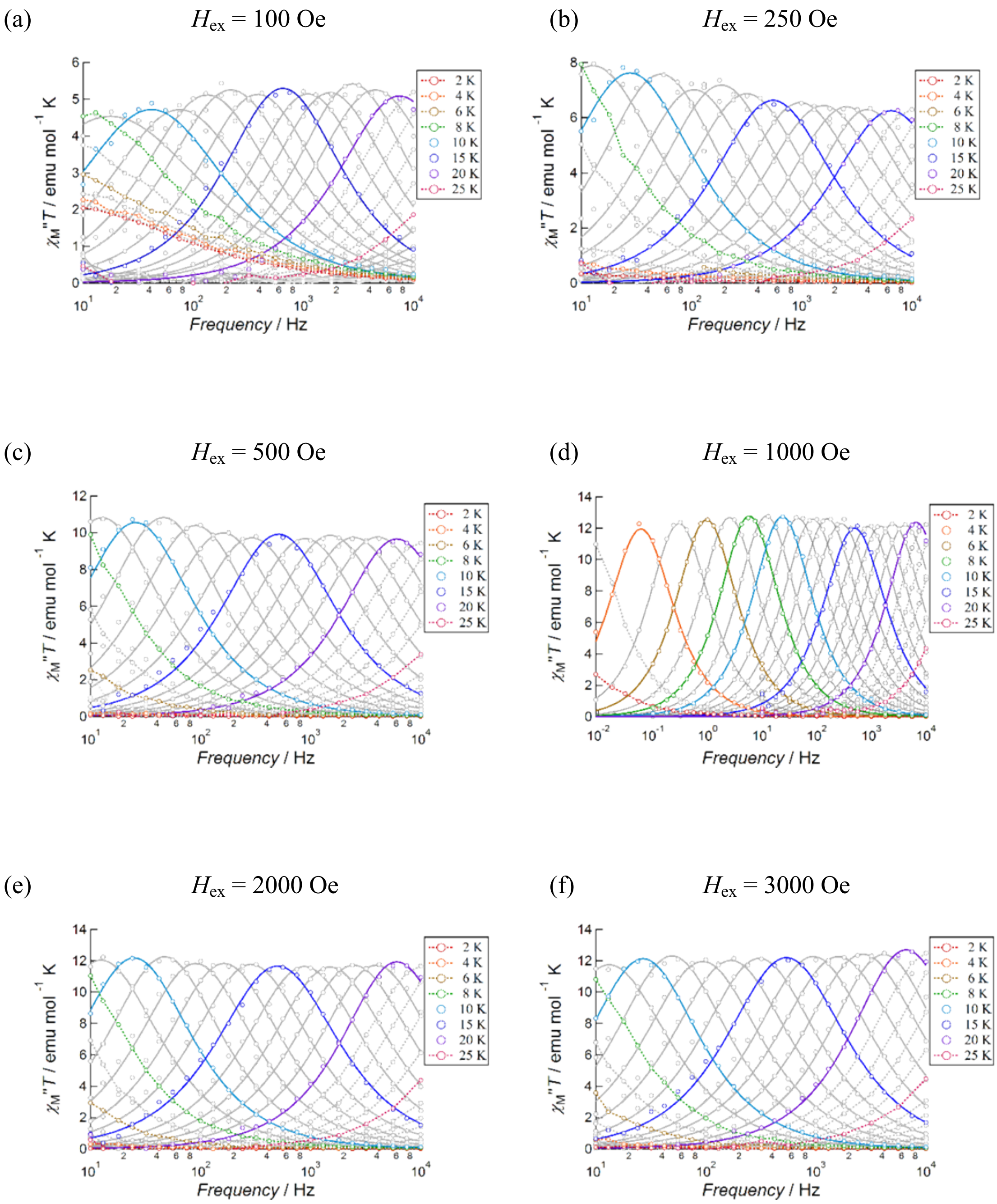

Figure S12 Frequency dependence of the product of χ_M'' and temperature of **5**, $\chi_M''T$, measured under 250-3000 Oe dc field. Solid curves represent the results of fits to a generalized Debye model, while the dotted curves are the guide for eyes.

(a) H_{ex} = 0 Oe

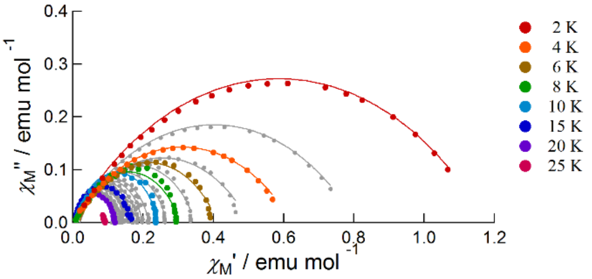

(b) H_{ex} = 100 Oe

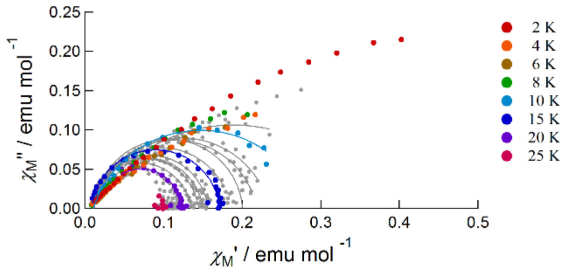

(c) H_{ex} = 250 Oe

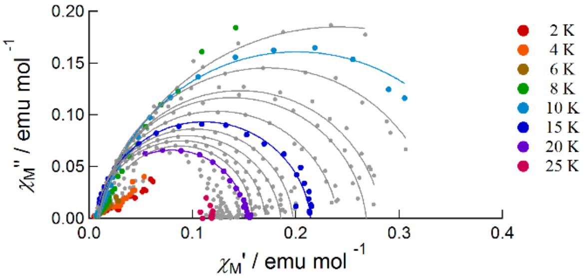

(d) H_{ex} = 500 Oe

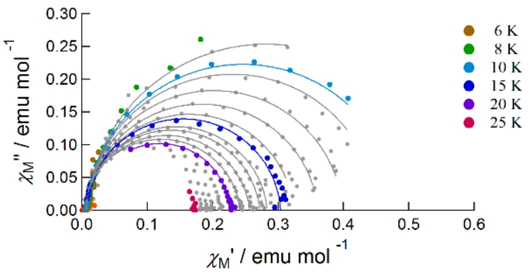

(e) H_{ex} = 1000 Oe

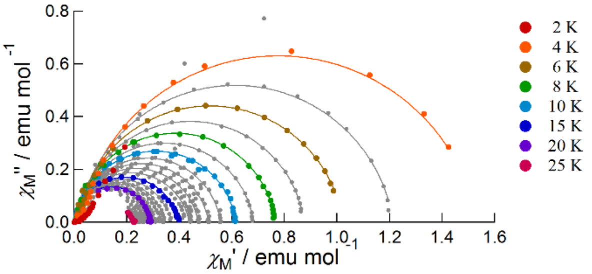

(f) H_{ex} = 2000 Oe

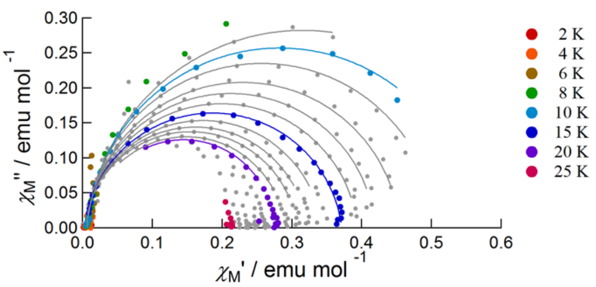

(g) H_{ex} = 3000 Oe

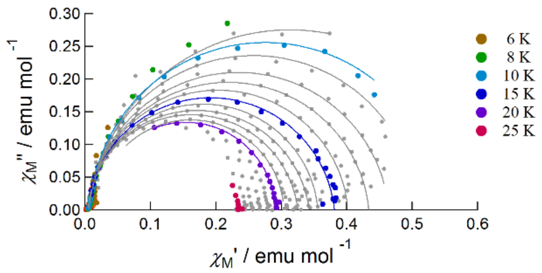

Figure S13 Cole-Cole plots of **5** measured under the application of external 0-3000 Oe dc field. Solid curves represent theoretical calculation on the basis of the generalized Debye model.

Table S2 Best fitted parameters of the extended Debye model for **5** under 0 Oe dc field.

T/K	χ_T / emu mol^{-1}	χ_S / emu mol^{-1}	τ / s	α
2.0	5.560(14)	0 *	0.0442(4)	0.4455(15)
3.0	3.819(10)	0 *	0.0405(3)	0.4516(11)
4.0	2.958(15)	0.0085(19)	0.0367(4)	0.452(3)
5.0	2.38(3)	0.05(2)	0.0298(9)	0.412(9)
6.0	1.96(3)	0.08(2)	0.0231(7)	0.335(15)
7.0	1.65(2)	0.09(2)	0.0151(5)	0.257(16)
8.0	1.427(15)	0.10(2)	0.0090(3)	0.190(9)
9.0	1.259(10)	0.100(15)	0.00516(12)	0.136(12)
10.0	1.131(6)	0.088(13)	0.00316(6)	0.104(10)
11.0	1.021(12)	0.049(10)	0.00176(5)	0.137(17)
12.0	0.933(8)	0.051(8)	0.00107(3)	0.102(15)
13.0	0.875(4)	0.042(4)	0.000659(10)	0.100(8)
14.0	0.810(3)	0.039(4)	0.000394(6)	0.078(8)
15.0	0.778(11)	0.030(7)	0.000241(7)	0.085(18)
16.0	0.748(8)	0.028(15)	0.000146(4)	0.112(16)
17.0	0.690(7)	0.025(10)	0.000087(3)	0.040(2)
18.0	0.659(8)	0.036(13)	0.000056(4)	0.061(12)
19.0	0.595(10)	0.021(7)	0.0000353(6)	0.038(6)
20.0	0.565(2)	0.017(6)	0.0000216(13)	0.063(5)

* fixed at 0 emu mol^{-1}

Table S3 Best fitted parameters of the extended Debye model for **5** under 1000 Oe dc field.

T/K	χ_T / emu mol^{-1}	χ_S / emu mol^{-1}	τ / s	α
4.0	7.27(7)	0.076(9)	2.63(6)	0.119(8)
5.0	5.75(4)	0.062(13)	0.527(5)	0.094(5)
6.0	4.83(4)	0.060(10)	0.1654(18)	0.086(6)
7.0	4.13(2)	0.053(10)	0.0628(7)	0.077(5)
8.0	3.618(15)	0.047(10)	0.0273(3)	0.072(5)
9.0	3.226(15)	0.042(12)	0.01319(12)	0.074(6)
10.0	2.909(15)	0.030(14)	0.00678(7)	0.079(6)
11.0	2.63(2)	0.023(18)	0.00350(5)	0.083(9)
12.0	2.42(2)	0.013(8)	0.00187(3)	0.089(9)
13.0	2.23(2)	0 *	0.00102(2)	0.090(5)
14.0	2.07(2)	0 *	0.000566(16)	0.106(15)
15.0	1.879(14)	0 *	0.000322(6)	0.104(11)
16.0	1.729(14)	0 *	0.000183(3)	0.086(6)
17.0	1.617(9)	0 *	0.0001073(18)	0.080(9)
18.0	1.538(13)	0 *	0.000065(2)	0.078(6)
19.0	1.462(6)	0 *	0.0000383(12)	0.084(6)
20.0	1.377(6)	0 *	0.0000241(15)	0.0692(8)

* fixed at 0 emu mol^{-1}

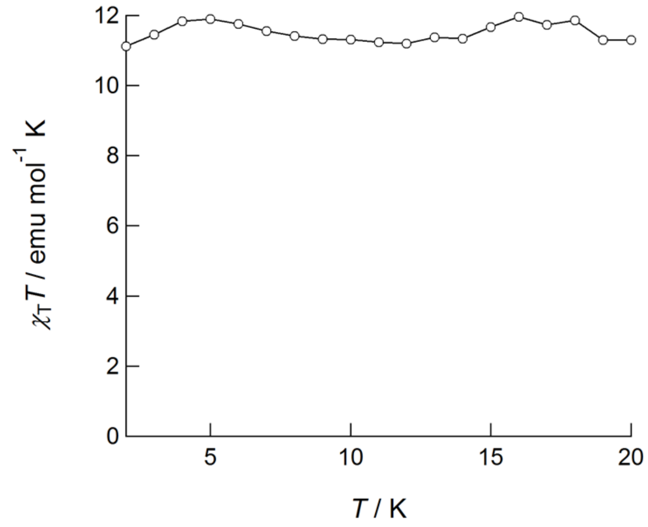

Figure S14 Temperature dependence of the product of the isothermal susceptibility χ_T and temperature T of **5** measured under 0 Oe dc field.

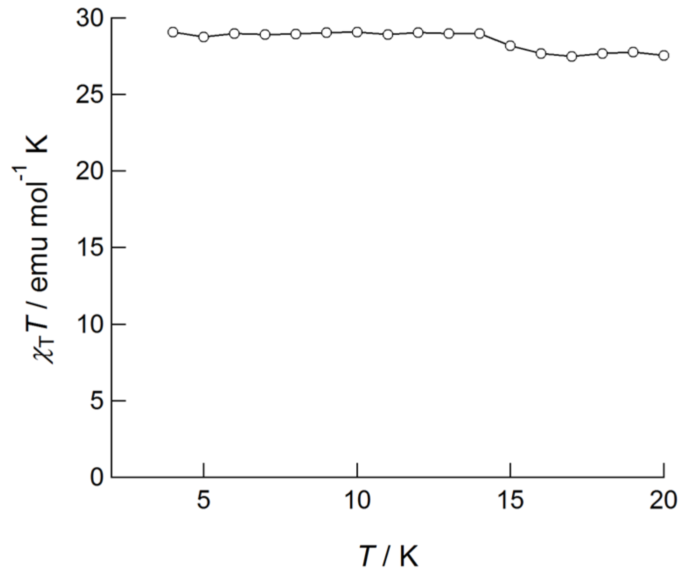

Figure S15 Temperature dependence of the product of the isothermal susceptibility χ_T and temperature T of **5** measured under 1000 Oe dc field.

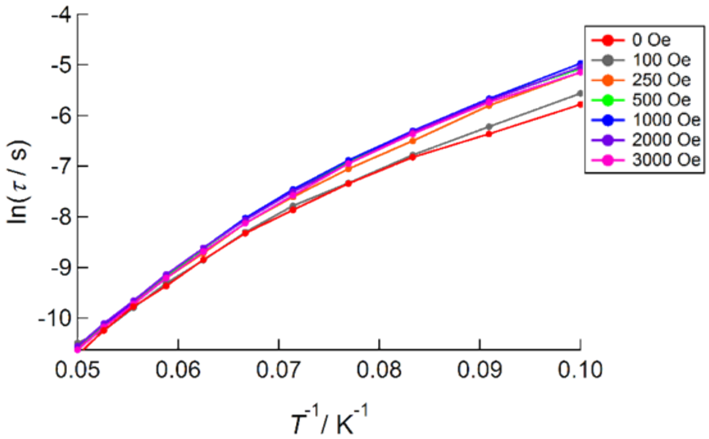

Figure S16 Dc field dependence of the Arrhenius plots for **5** measured under dc field ranging from 0 Oe to 3000 Oe.

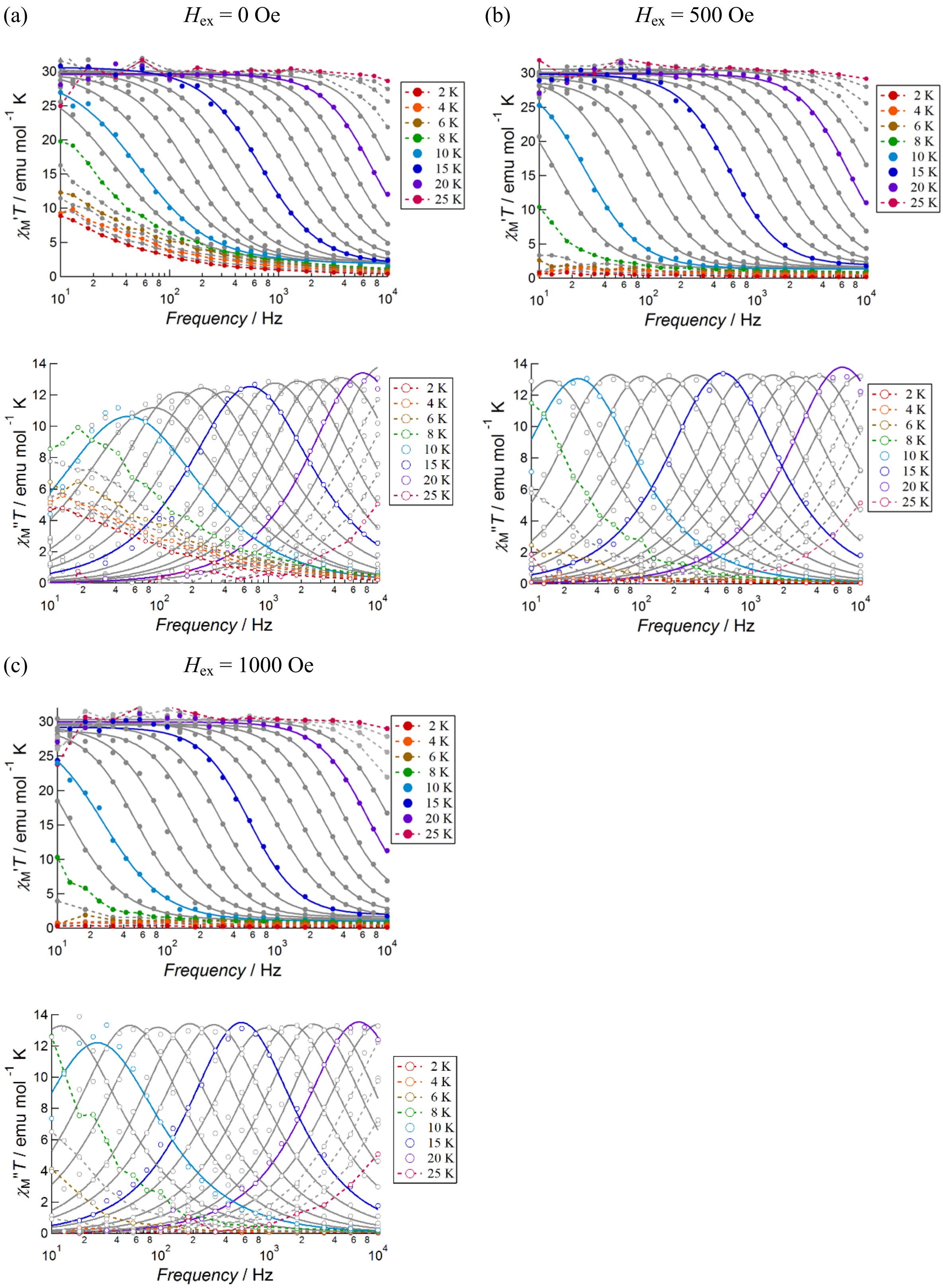

Figure S17 Frequency dependence of the products of $\chi_M'T$ (closed circles) and $\chi_M''T$ (open circles) of $[Dy_{0.07}La_{0.93}(NO_3)\{Zn(L)(SCN)\}_2]$ (**5'**) in type-A structure, measured under 0-1000 Oe dc field. Solid curves represent theoretical calculations on the basis of the generalized Debye model, whereas dotted curves serve as guides for the eyes.